

ELECTRON SPIN RESONANCE STUDY OF THE E'_2
CENTER IN QUARTZ

By

MAHENDRAKUMAR G. JANI
"

Bachelor of Science

Gujarat University

Ahmedabad, India

1976

submitted to the Faculty of the Graduate College
of the Oklahoma State University
in partial fulfillment of the requirements
for the Degree of
MASTER OF SCIENCE
May, 1979

Thesis
1979
J33e
wp2



ELECTRON SPIN RESONANCE STUDY OF THE E'_2
CENTER IN QUARTZ

Thesis Approved:

Larry E. Halliburton

Thesis Adviser

E. K. ...

W. A. Sibley

Norman N. Durbin

Dean of the Graduate College

1029392

ACKNOWLEDGMENTS

The author wishes to thank Dr. L. E. Halliburton for his guidance, assistance and understanding. Without his help, this work would not have been completed. Appreciation is expressed to Dr. W. A. Sibley and Dr. E. E. Kohnke for serving on his Committee. Appreciation is also expressed to R. A. Weeks for kindly providing the quartz sample used in this study.

The author wishes to thank his parents, Pragna, Rahul and Shailesh, for their love, affection and encouragement. The author also wishes to thank Sauwane for her love, affection and moral support. Thanks are extended to Ms. Janet Sallee for typing this manuscript.

Financial support from the U.S. Air Force under contract number F 19628-77-C-0171 for Summer 1978 and the Physics Department at Oklahoma State University is gratefully acknowledged.

TABLE OF CONTENTS

Chapter	Page
I. INTRODUCTION.	1
R. A. Weeks and C. M. Nelson (3)	3
R. H. Silsbee (5).	3
Kwok Leung Yip and W. Beall Fowler (6)	5
R. A. Weeks (7).	5
F. J. Feigl and J. H. Anderson (8)	6
L. E. Halliburton and J. A. Weil (9)	6
Present Study.	6
II. EXPERIMENTAL PROCEDURE.	8
I. Sample Preparation and Defect Production	8
II. ESR Spectrometer.	9
III. THEORETICAL ANALYSIS AND EXPERIMENTAL RESULTS	12
I. Theoretical Analysis	12
II. Experimental Results.	19
IV. DISCUSSION.	32
SELECTED BIBLIOGRAPHY.	34
APPENDIX A	35
APPENDIX B	41

LIST OF TABLES

Table	Page
I. The Lower Half of the Hamiltonian Matrix.	18
II. Spin Hamiltonian Parameters for the E_2' Center From Present Study	29
III. Spin Hamiltonian Parameters Reported by Feigl and Anderson.	30

LIST OF FIGURES

Figure	Page
1. The Crystal Structure of α -Quartz.	2
2. Different E'-Type Center Models.	4
3. ESR Spectrometer	10
4. ESR Spectrum for the E' ₂ and the E' ₄ Center With Magnetic Field Along the [001] Direction at 300K.	20
5. ESR Spectrum for ²⁹ Si Hyperfine Interaction With Magnetic Field Along the [001] Direction at 300K.	21
6. Angular Dependence for ²⁹ Si Hyperfine Interaction.	23
7. Angular Dependence for the High Field Doublet Illustrating the Proton Effects	24
8. Pulse Anneal Study of the E' ₂ and the E' ₄ Center in SiO ₂	25
9. Energy Levels and Possible Transitions in an S = 1/2, I ₁ = 1/2 and I ₂ = 1/2 System.	27

CHAPTER I

INTRODUCTION

Radiation-induced defects in solids have been studied extensively for the last sixty years. It is well known that high energy irradiation produces defects in crystals. Study of these defects is important since many materials are being used in various industrial areas involving high energy irradiation.

Electron spin resonance has been used as one of the important tools to visualize the crystalline environment in the vicinity of well-localized defects (called point defects) in crystalline solids.

Quartz (SiO_2) is different from other oxides, in that it is neither completely ionic nor completely covalent. This makes its study much more difficult. It does not have a high symmetry crystal structure (1). The crystal structure for SiO_2 is shown in Figure 1. For quite some time now quartz has been used for oscillators in space satellites and hence has been exposed to various kinds of irradiation in outer space. It has been observed that properties of the oscillators do not remain the same as a consequence of its exposure to high energy irradiation (2).

The E' center in quartz is similar to the F center in ionic materials in which an electron is trapped at a negative ion vacancy. The notation was first introduced by R. A. Weeks and C. M. Nelson (3) for this paramagnetic defect in quartz. There are three different

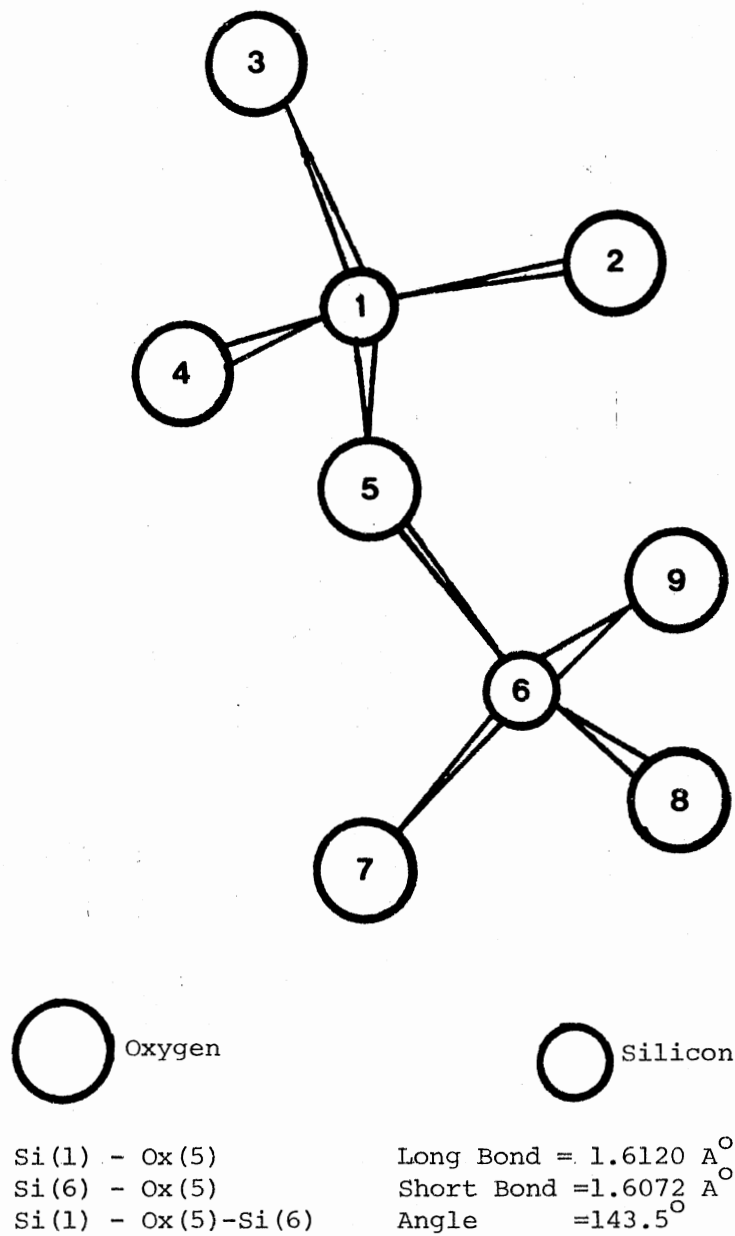


Figure 1. Structure of Right Quartz. (Projection on z-plane with +z axis coming out of plane of paper)

types of E' centers reported in the literature. They are the E'₁' center, the E'₂' center and the E'₄' center. Some E' type centers are shown in Figure 2. The E'₂' and E'₄' centers are different from the E'₁' center in that proton hyperfine effects are associated with them.

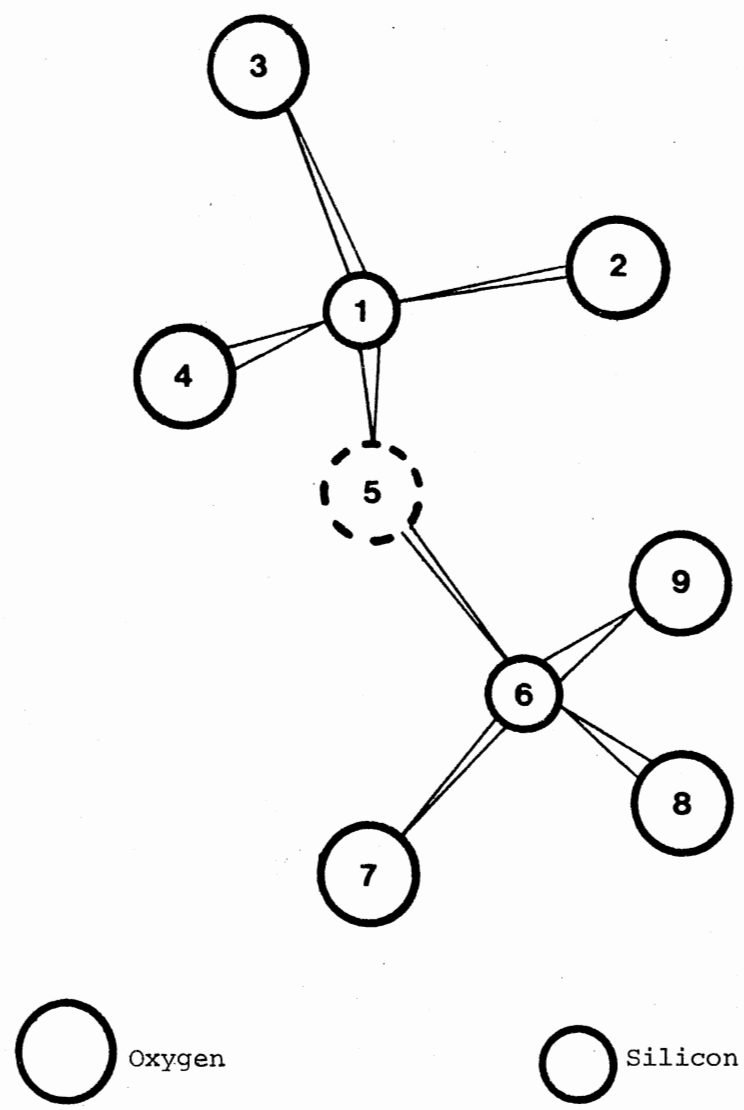
The E'₁' center was originally reported by R. A. Weeks (4). This study inspired many other people to carry out theoretical and experimental investigations of the E' centers in SiO₂. Some of these studies are discussed briefly in the following few paragraphs.

R. A. Weeks and C. M. Nelson (3)

The correlation of optical bands with ESR spectra was established by a series of optical bleaching and thermal annealing experiments. They used ⁶⁰Co γ-irradiated synthetic crystalline quartz in this study. It was concluded from this study that an optical band at 210 nm is associated with the E'₁' center and an absorption band at 230 nm is associated with the E'₂' center. Defect models were proposed for the E'₁', the E''₁ and the E'₂' centers.

R. H. Silsbee (5)

A detailed electron spin resonance study of E'₁' centers produced by fast neutron-irradiation of crystalline quartz was done. The parameters for the g tensor and hyperfine tensor were reported for the E'₁' center. It was concluded that the E'₁' center, produced by low neutron doses, consisted of an unpaired electron in a non-bonding orbital on a silicon. The complete breakdown of the crystalline structure was observed at high doses of neutron irradiation. A pair of weak lines 400



- E_1 - Contains no electrons
- E'_1 - Trapped a single electron
- E''_1 - Trapped two electrons

Figure 2. Different E'-Type Center Models

gauss apart were attributed to a single ^{29}Si strong hyperfine interaction.

Kwok Leung Yip and W. Beall Fowler (6)

Theoretical analysis of the E'_1 center in the α -quartz structure of SiO_2 was done using a linear combination of localized orbital-molecular orbital (LCLO-MO) cluster method. Similar analysis was also done for the $E'_1(\text{Ge})$ center which is an electron trapped by a germanium ion substituted for a silicon ion neighboring an oxygen vacancy in SiO_2 . It was also concluded from this theoretical study that the E'_1 center is an electron trapped at an oxygen vacancy. The trapped electron at the defect site is strongly localized in a non-bonding sp^3 hybrid orbital centered on silicon (or Ge substituted for Si) and oriented almost along a Si-O short bond direction toward the oxygen vacancy.

R. A. Weeks (7)

The E'_2 center was studied in detail using the electron spin resonance technique. A spectrum consisting of two lines about 0.4 ± 0.1 gauss apart was observed for the magnetic field oriented along the c axis. An angular dependence study was done for this spectrum and the g tensor parameters were calculated. It was concluded from this study that the E'_2 center is an electron trapped at an oxygen vacancy with a proton nearby. In addition to the primary doublet spectrum, an additional pair of similar doublets about 412 gauss apart was observed for the magnetic field along the c axis. The widely split pair of doublets was attributed to the strong hyperfine interaction with ^{29}Si .

F. J. Feigl and J. H. Anderson (8)

Paramagnetic defects produced by low energy ionizing radiation in crystalline quartz doped with Ge were studied through electron spin resonance. Their analysis indicated that these defects are similar to the E'_1 and the E'_2 centers in pure crystalline quartz, with a Ge ion substituted for the central Si ion in the E'-defect structures. The parameters for these Ge-related defects were calculated and compared with the parameters reported by R. H. Silsbee (5) and R. A. Weeks (7). It was concluded from this investigation that the unpaired electron occupies a non-bonding orbital strongly localized on the Ge impurity. A single oxygen vacancy model for the entire E' class of center was adequate to explain their data.

L. E. Halliburton and J. A. Weil (9)

The E'_4 center first reported by R. A. Weeks and C. M. Nelson (3), was studied in detail using electron spin resonance. Nelson and Weeks suggested that the four equally spaced and equally intense line spectrum was a result of an unpaired electron interacting with an alkali ion ($I = 3/2$). The complete angular dependence study of the four line spectrum was done and the parameters for the g tensor and A tensors were calculated. It was concluded from this study that the E'_4 center has $S = 1/2$ and the hyperfine structure arises from interactions with a proton ($I = 1/2$) in a situation permitting observation of all $2S(2I+1)^2$ possible ESR transitions.

Present Study

In the present study, the angular dependence study of the two

pairs of lines due to strong hyperfine interaction with ^{29}Si for the E'_2 center is reported. This study provides additional information from which the precise model for the E'_2 center in quartz may be determined.

CHAPTER II

EXPERIMENTAL PROCEDURE

In this chapter, the experimental procedure and equipment used to study the E'_2 center in SiO_2 is described. In Section I, sample preparation and defect production in SiO_2 is discussed. The ESR spectrometer and operating procedure is outlined in Section II.

I. Sample Preparation and Defect Production

The sample used in this study was obtained from R. A. Weeks, Oak Ridge National Laboratory. The main difficulty in this study was that the history of treatments received by this sample was not available. It was known that the crystal had been irradiated in a ^{60}Co γ -cell, receiving a dosage of 4.5×10^9 R at some time in the past.

The next important question was how one explains defect production in the crystal. One of the possible explanations is that oxygen vacancies were already present in the crystal as a result of the hydrothermal growth process. This seems reasonable, since it was observed that Sawyer Electronic Grade samples, on being irradiated by electrons from a Van de Graaff accelerator, give similar ESR signals as from our γ -irradiated samples. Dimensions of the Sawyer Electronic Grade sample were nearly one-half of our γ -irradiated samples. The irradiation dose received by our Sawyer samples is not sufficient to create oxygen vacancies. Hence we conclude that oxygen vacancies are initially pres-

ent in the sample. Electron irradiation or γ -irradiation just moves around the charges to form paramagnetic defects.

II. ESR Spectrometer

The x-band homodyne spectrometer used to obtain the ESR spectra in this study is shown in the block diagram in Figure 3. The microwave power was supplied by a Varian VA-153C klystron. The klystron was locked to the resonant frequency of the sample cavity with the help of a reflector-modulated stabilizer. The sample was placed inside a rectangular microwave cavity operating in the TE_{102} mode. The precision attenuator in the sample arm regulated the microwave power incident on the sample. The microwave frequency was measured using a Hewlett-Packard frequency counter.

A Varian 9-inch V-7200 electro-magnet was used to produce the magnetic field. Any variations in the field intensity were detected by a Hall probe mounted on one of the pole caps. This probe supplies an error signal which adjusts the magnet current to maintain stability of the field. Magnetic field values could be directly read in gauss from the field set controls. But this method was not precise enough to yield correct field values, thus a different method was used.

The static magnetic field was amplitude modulated at 100 kHz. The modulation coils were mounted on the outside of a glass Dewar. The microwave signal was detected using a properly biased low-noise Schottky barrier diode. This signal was then amplified by a broad-band amplifier (Micro-Now Instruments Co., Model 521). The amplified signal was fed to a phase sensitive detector (PAR Model 128) which greatly enhanced the signal-to-noise ratio. The reference signal for the phase sensitive

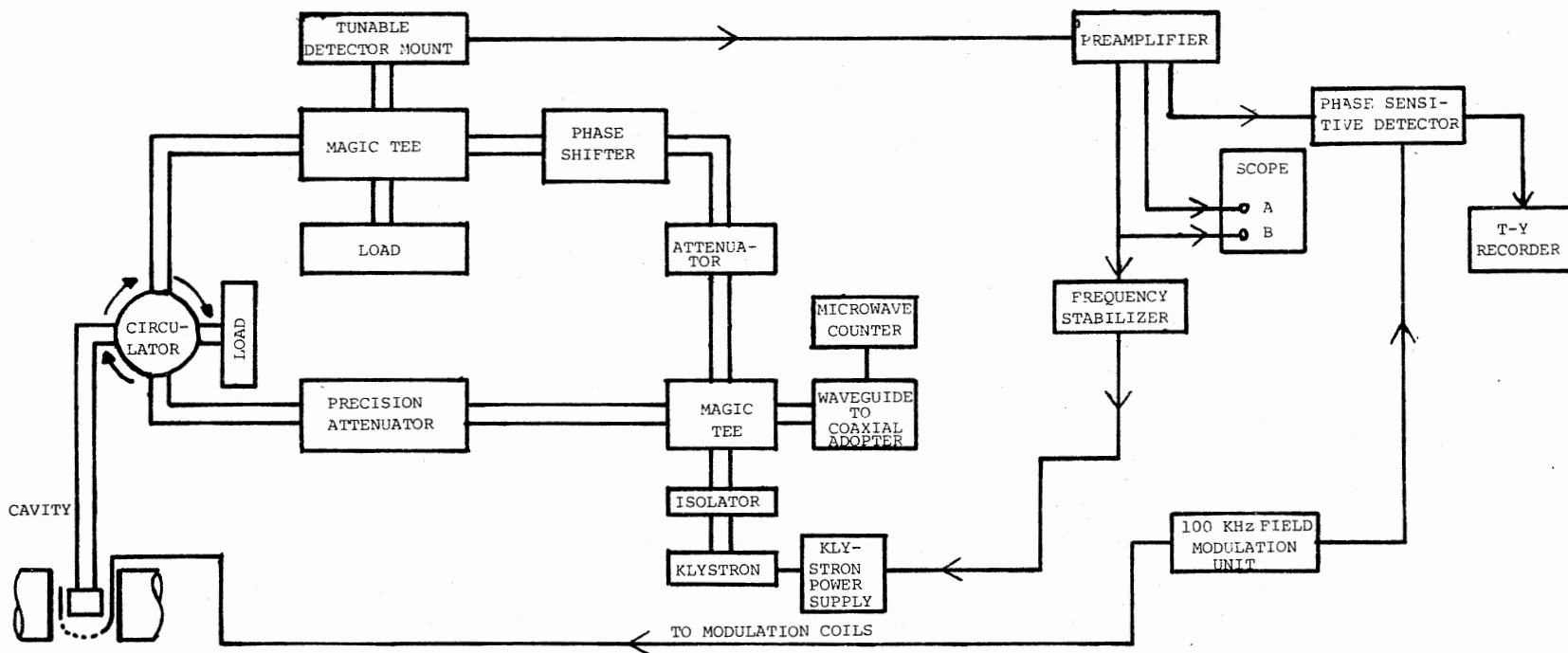


Figure 3. ESR Spectrometer

detector was obtained from the oscillator which amplitude-modulated the magnetic field. The output from the phase sensitive detector was fed into a strip chart recorder (Leeds and Northrup) which yielded a first derivative ESR spectrum.

Magnetic field measurements were made using an NMR marginal oscillator and proton probe. The probe essentially consisted of coaxial cable surrounded by a brass tube. At one end of the probe a rigid BNC connector was provided for connecting to the marginal oscillator. At the other end of the coaxial cable an inductor which consisted of 18-20 turns of copper wire was wound on a glass capsule containing the NMR sample. Since the probe could not be placed at the same position as the ESR sample in the cavity, a correction was made to the measured field values using a standard Cr^{3+} -doped MgO sample whose g-value is 1.9799.

CHAPTER III

THEORETICAL ANALYSIS AND EXPERIMENTAL RESULTS

This chapter is divided into two sections. The theoretical format for analysis of the E'_2 center spectra is presented in Section I. Experimental results and computer programs for data reduction are discussed in Section II. Some of the results obtained using these computer programs are also presented in Section II. Conclusions reached in this study will be presented in the next chapter.

I. Theoretical Analysis

The spin Hamiltonian describing the E'_2 center is given by

$$H = \vec{H} \cdot \vec{g} \cdot \vec{S} + \vec{I}_1 \cdot \vec{A}_1 \cdot \vec{S} + \vec{I}_2 \cdot \vec{A}_2 \cdot \vec{S} - (g_N \beta_N)_1 \vec{H} \cdot \vec{I}_1 - (g_N \beta_N)_2 \vec{H} \cdot \vec{I}_2$$

where the first term represents the electron Zeeman interaction, the second and the third terms represent hyperfine interactions due to a proton (H^+) nucleus and a ^{29}Si ($I = 1/2$, 4.7% abundant) nucleus, respectively, with the unpaired electron. The last two terms represent nuclear Zeeman interactions for the two nuclei, respectively.

The following coordinate systems are used in converting the Hamiltonian to a suitable form for computer programming.

x, y, z : Magnetic field coordinate system chosen such that the magnetic field is along the z direction.

x_c, y_c, z_c : Crystal coordinate system.

x_g, y_g, z_g : Principal axes of the g tensor.

x_1, y_1, z_1 : Principal axes system for the proton hyperfine tensor,
 \leftrightarrow
 A_1 .

x_2, y_2, z_2 : Principal axes system for the ^{29}Si hyperfine tensor,
 \leftrightarrow
 A_2 .

Rewriting the Hamiltonian in terms of different coordinate systems,

we have

$$\begin{aligned}
 H = & \beta [S_{x_g} g_x H_{x_g} + S_{y_g} g_y H_{y_g} + S_{z_g} g_z H_{z_g}] \\
 & + I_{x_1} A_{x_1} S_{x_1} + I_{y_1} A_{y_1} S_{y_1} + I_{z_1} A_{z_1} S_{z_1} \\
 & + I_{x_2} A_{x_2} S_{x_2} + I_{y_2} A_{y_2} S_{y_2} + I_{z_2} A_{z_2} S_{z_2} \\
 & - (g_N \beta_N)_1 H I_{z_1} - (g_N \beta_N)_2 H I_{z_2}
 \end{aligned}$$

The relationships between the different coordinate systems are

$$\begin{pmatrix} x_g \\ y_g \\ z_g \end{pmatrix} = [TG] \begin{pmatrix} x \\ y \\ z \end{pmatrix},$$

$$\begin{pmatrix} x_1 \\ y_1 \\ z_1 \end{pmatrix} = [TH] \begin{pmatrix} x \\ y \\ z \end{pmatrix},$$

and

$$\begin{pmatrix} x_2 \\ y_2 \\ z_2 \end{pmatrix} = [\text{TM}] \begin{pmatrix} x \\ y \\ z \end{pmatrix}$$

where the transformation matrices are defined as follows:

[G]: Transforms principal axes of the g tensor to crystal coordinate system.

[H]: Transforms principal axes of the hyperfine tensor A_1 to crystal coordinate system.

[M]: Transforms principal axes of the hyperfine tensor A_2 to crystal coordinate system.

[R]: Transforms the crystal coordinate system to the magnetic field coordinate system.

[TG] = [G] [R]: Transforms principal axes of the g tensor to the magnetic field coordinate system.

[TH] = [H] [R]: Transforms principal axes system of hyperfine tensor A_1 to the magnetic field coordinate system.

[TM] = [M] [R]: Transforms principal axes system of hyperfine tensor A_2 to the magnetic field coordinate system.

Now using the above transformations, the Hamiltonian is written in terms of the magnetic field coordinate system only, as follows:

$$\begin{aligned}
H = & w1 S_x + w2 S_y + w3 S_z + w4 I_{1x} S_x + w5 I_{1x} S_y \\
& + w6 I_{1x} S_z + w5 I_{1y} S_x + w7 I_{1y} S_y + w8 I_{1y} S_z \\
& + w6 I_{1z} S_x + w8 I_{1z} S_y + w9 I_{1z} S_z + w10 I_{2x} S_x \\
& + w11 I_{2x} S_y + w12 I_{2x} S_z + w11 I_{2y} S_x + w13 I_{2y} S_y \\
& + w14 I_{2y} S_z + w12 I_{2z} S_x + w14 I_{2z} S_y + w15 I_{2z} S_z \\
& - (g_{NN}^1 \beta_N) HI_{1z} - (g_{NN}^2 \beta_N) HI_{2z}
\end{aligned}$$

where

$$w1 = \beta H [g_x TG(1,1)TG(1,3) + g_y TG(2,1)TG(2,3) + g_x TG(3,1)TG(3,3)]$$

$$w2 = \beta H [g_x TG(1,2)TG(1,3) + g_y TG(2,2)TG(2,3) + g_z TG(3,2)TG(3,3)]$$

$$w3 = \beta H [g_x TG(1,3)TG(1,3) + g_y TG(2,3)TG(2,3) + g_z TG(3,3)TG(3,3)]$$

$$w4 = A_{1x} TH(1,1)TH(1,1) + A_{1y} TH(2,1)TH(2,1) + A_{1z} TH(3,1)TH(3,1)$$

$$w5 = A_{1x} TH(1,1)TH(1,2) + A_{1y} TH(2,1)TH(2,2) + A_{1z} TH(3,1)TH(3,2)$$

$$w6 = A_{1x} TH(1,1)TH(1,3) + A_{1y} TH(2,1)TH(2,3) + A_{1z} TH(3,1)TH(3,3)$$

$$w7 = A_{1x} TH(1,2)TH(1,2) + A_{1y} TH(2,2)TH(2,2) + A_{1z} TH(3,2)TH(3,2)$$

$$w8 = A_{1x} TH(1,2)TH(1,3) + A_{1y} TH(2,2)TH(2,3) + A_{1z} TH(3,2)TH(3,3)$$

$$w9 = A_{1x} TH(1,3)TH(1,3) + A_{1y} TH(2,3)TH(2,3) + A_{1z} TH(3,3)TH(3,3)$$

$$w10 = A_{2x} TM(1,1)TM(1,1) + A_{2y} TM(2,1)TM(2,1) + A_{2z} TM(3,1)TM(3,1)$$

$$w11 = A_{2x} TM(1,1)TM(1,2) + A_{2y} TM(2,1)TM(2,2) + A_{2z} TM(3,1)TM(3,2)$$

$$w12 = A_{2x} TM(1,1)TM(1,3) + A_{2y} TM(2,1)TM(2,3) + A_{2z} TM(3,1)TM(3,3)$$

$$w13 = A_{2x} TM(1,2)TM(1,2) + A_{2y} TM(2,2)TM(2,2) + A_{2z} TM(3,2)TM(3,2)$$

$$w14 = A_{2x} TM(1,2)TM(1,3) + A_{2y} TM(2,2)TM(2,3) + A_{2z} TM(3,2)TM(3,3)$$

$$w15 = A_{2x} TM(1,3)TM(1,3) + A_{2y} TM(2,3)TM(2,3) + A_{2z} TM(3,3)TM(3,3)$$

Using the raising and the lowering operators

$$S_+ = S_x + iS_y, \quad S_- = S_x - iS_y,$$

$$I_+ = I_x + iI_y, \quad I_- = I_x - iI_y,$$

we can write the Hamiltonian in the following form,

$$\begin{aligned} H = & W3 S_z + W9 I_{1z} S_z + W15 I_{2z} S_z - (g_N \beta_N) H I_{1z} \\ & - (g_N \beta_N) H I_{2z} + Q1 S_+ + Q1 S_- + Q2 I_{1+} S_+ \\ & + Q3 I_{1+} S_- + Q3 I_{1-} S_+ + Q2 I_{1-} S_- + Q4 I_{1+} S_z \\ & + Q4 I_{1-} S_z + Q4 I_{1z} S_+ + Q4 I_{1z} S_- + Q5 I_{2+} S_+ \\ & + Q6 I_{2+} S_- + Q6 I_{2-} S_+ + Q5 I_{2-} S_- + Q7 I_{2+} S_z \\ & + Q7 I_{2-} S_z + Q7 I_{2z} S_+ + Q7 I_{2z} S_- \end{aligned}$$

where

$$Q1 = 1/2(W1 + iW2)$$

$$Q2 = 1/4(W4 - W7) + 1/2 W5$$

$$Q3 = 1/4(W4 + W7)$$

$$Q4 = 1/2(W6 + iW8)$$

$$Q5 = 1/4(W10 - W13) + 1/2 W11$$

$$Q6 = 1/4(W10 + W13)$$

$$Q7 = 1/2(W12 + iW14) .$$

Since the ^{29}Si nucleus has $I = 1/2$ and the proton (H^+) nucleus has $I = 1/2$, the basis set chosen is $|M_S = \pm 1/2, M_{I_1} = \pm 1/2, M_{I_2} = \pm 1/2\rangle$. This basis set consists of eight vectors, which allows one to write the Hamiltonian in an 8×8 matrix form. The Hamiltonian being hermitian, the lower half of the matrix elements are sufficient to calculate the

energy eigenvalues.

The notation for the lower half of the matrix elements is presented in Table I. The non-zero elements are given as follows:

$$A(1,1) = 1/2 W3 + 1/4 (W9+W15) - 1/2 (g_{N^N}^{\beta_1})_1 H - 1/2 (g_{N^N}^{\beta_2})_2 H$$

$$A(2,1) = 1/2 Q4$$

$$A(3,1) = Q1 + 1/2 (Q4+Q7)$$

$$A(4,1) = Q2$$

$$A(5,1) = 1/2 Q7$$

$$A(7,1) = Q5$$

$$A(2,2) = 1/2 W3 - 1/4 (W9-W15) + 1/2 (g_{N^N}^{\beta_1})_1 H - 1/2 (g_{N^N}^{\beta_2})_2 H$$

$$A(3,2) = Q3$$

$$A(4,2) = Q1 - 1/2 (Q4-Q7)$$

$$A(6,2) = 1/2 Q7$$

$$A(8,2) = Q5$$

$$A(3,3) = - 1/2 W3 - 1/4 (W9+W15) - 1/2 (g_{N^N}^{\beta_1})_1 H - 1/2 (g_{N^N}^{\beta_2})_2 H$$

$$A(4,3) = - 1/2 Q4$$

$$A(5,3) = Q6$$

$$A(7,3) = - 1/2 Q7$$

$$A(4,4) = - 1/2 W3 + 1/4 (W9-W15) + 1/2 (g_{N^N}^{\beta_1})_1 H - 1/2 (g_{N^N}^{\beta_2})_2 H$$

$$A(6,4) = Q6$$

$$A(8,4) = - 1/2 Q7$$

$$A(5,5) = 1/2 W3 + 1/4 (W9-W15) - 1/2 (g_{N^N}^{\beta_1})_1 H + 1/2 (g_{N^N}^{\beta_2})_2 H$$

$$A(6,5) = 1/2 Q4$$

$$A(7,5) = Q1 + 1/2 (Q4-Q7)$$

$$A(8,5) = Q2$$

TABLE I
THE LOWER HALF OF THE HAMILTONIAN MATRIX

	$ \frac{1}{2}, \frac{1}{2}, \frac{1}{2}\rangle$	$ \frac{1}{2}, -\frac{1}{2}, \frac{1}{2}\rangle$	$ \frac{1}{2}, \frac{1}{2}, \frac{1}{2}\rangle$	$ \frac{1}{2}, -\frac{1}{2}, \frac{1}{2}\rangle$	$ \frac{1}{2}, \frac{1}{2}, -\frac{1}{2}\rangle$	$ \frac{1}{2}, -\frac{1}{2}, -\frac{1}{2}\rangle$	$ \frac{1}{2}, \frac{1}{2}, -\frac{1}{2}\rangle$	$ \frac{1}{2}, -\frac{1}{2}, -\frac{1}{2}\rangle$
$ \frac{1}{2}, \frac{1}{2}, \frac{1}{2}\rangle$	A(1,1)							
$ \frac{1}{2}, -\frac{1}{2}, \frac{1}{2}\rangle$	A(2,1)	A(2,2)						
$ \frac{1}{2}, \frac{1}{2}, \frac{1}{2}\rangle$	A(3,1)	A(3,2)	A(3,3)					
$ \frac{1}{2}, -\frac{1}{2}, \frac{1}{2}\rangle$	A(4,1)	A(4,2)	A(4,3)	A(4,4)				
$ \frac{1}{2}, \frac{1}{2}, -\frac{1}{2}\rangle$	A(5,1)	0	A(5,3)	0	A(5,5)			
$ \frac{1}{2}, -\frac{1}{2}, -\frac{1}{2}\rangle$	0	A(6,2)	0	A(6,4)	A(6,5)	A(6,6)		
$ \frac{1}{2}, \frac{1}{2}, -\frac{1}{2}\rangle$	A(7,1)	0	A(7,3)	0	A(7,5)	A(7,6)	A(7,7)	
$ \frac{1}{2}, -\frac{1}{2}, -\frac{1}{2}\rangle$	0	A(8,2)	0	A(8,4)	A(8,5)	A(8,6)	A(8,7)	A(8,8)

$$A(6,6) = 1/2 W_3 - 1/4 (W_9+W_{15}) + 1/2 (g_{N_1} \beta_{N_1})_1 H + 1/2 (g_{N_2} \beta_{N_2})_2 H$$

$$A(7,6) = Q_3$$

$$A(8,6) = Q_1 - 1/2 (Q_4 + Q_7)$$

$$A(7,7) = - 1/2 W_3 - 1/4 (W_9-W_{15}) - 1/2 (g_{N_1} \beta_{N_1})_1 H + 1/2 (g_{N_2} \beta_{N_2})_2 H$$

$$A(8,7) = - 1/2 Q_4$$

$$A(8,8) = - 1/2 W_3 + 1/4 (W_9+W_{15}) + 1/2 (g_{N_1} \beta_{N_1})_1 H + 1/2 (g_{N_2} \beta_{N_2})_2 H$$

II. Experimental Results

The principal E'_2 center ESR spectrum for the magnetic field along the [001] direction consists of two equally intense lines 0.37 ± 0.02 gauss apart as shown in Figure 4. The other four lines in the figure represent the E'_4 center. This data was obtained at 300K. The lowest field E'_4 center line was used to check the alignment. The two lines associated with the E'_2 center arise as a result of the interaction of an electron trapped at an oxygen vacancy with a proton near the defect site (3).

In addition to this primary doublet for the E'_2 center, two additional weak pairs of lines were observed with the magnetic field along the [001] direction as shown in Figure 5. The separation of each of these pairs of lines is nearly 0.37 ± 0.02 gauss, the same as the primary doublet. One pair of lines was approximately 198.6 gauss above the primary doublet and the other pair was nearly 226.8 gauss below the primary doublet. The separation between these two pairs of doublets is 425.4 gauss which is greater than the value 412 gauss reported in the literature by R. A. Weeks [7]. These low and high field pairs of doublets are attributed to a strong hyperfine interaction with a ^{29}Si

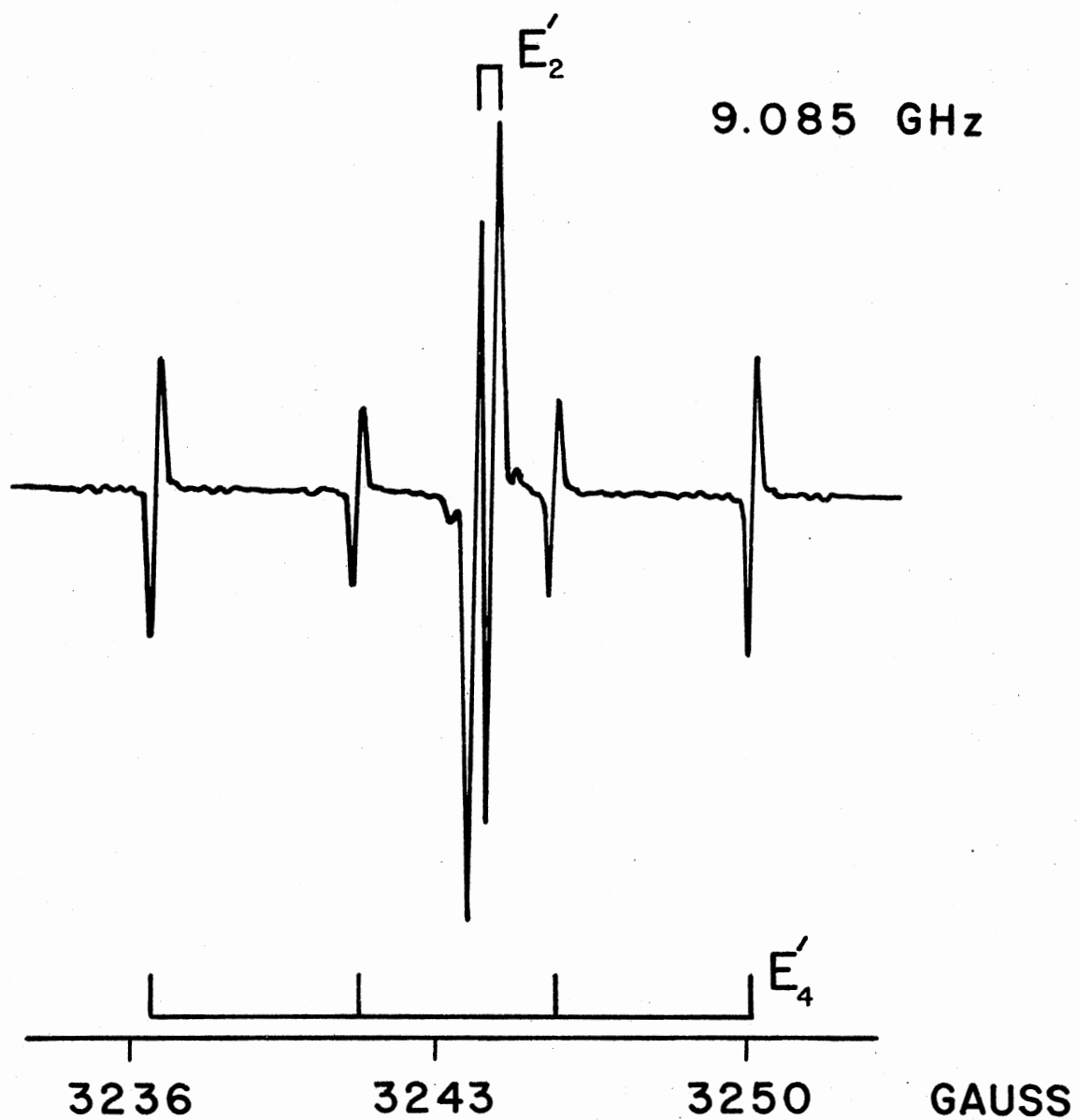


Figure 4. ESR Spectrum for the E'_2 and the E'_4 Center With Magnetic Field Along the [001] Direction at 300K

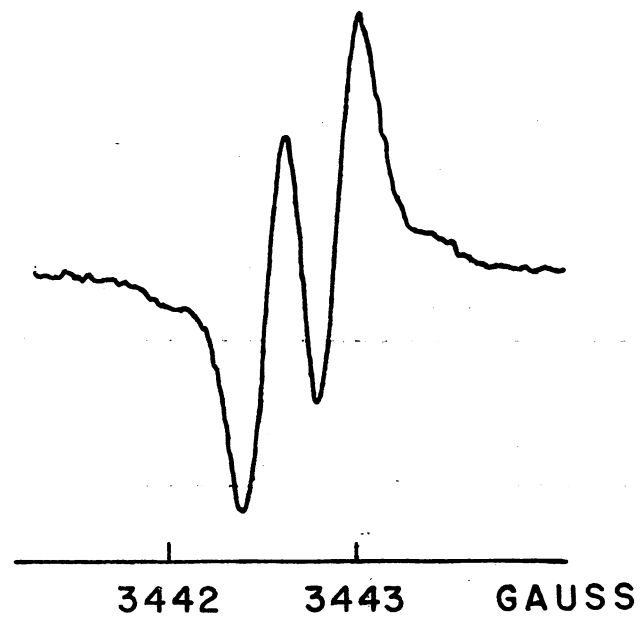
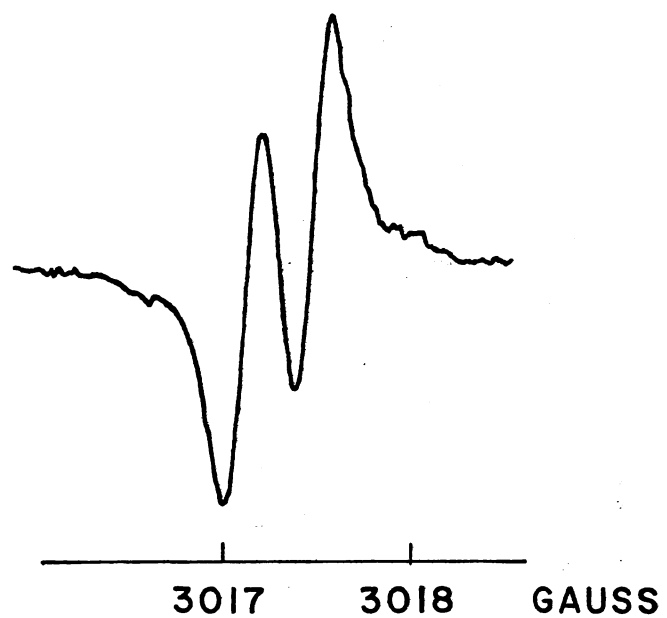


Figure 5. ESR Spectrum for ^{29}Si Hyperfine Interaction With Magnetic Field Along the [001] Direction at 300 K.

nucleus ($I = \frac{1}{2}$, 4.7% natural abundance).

An angular dependence study of the low and high field pairs of doublets was carried out at 300K. The magnetic field was rotated about the two-fold crystal axis and spectra were obtained at 15° intervals. Data were taken up to 70° of rotation on each side from the [001] direction. The intensity of the signal dropped rapidly beyond 70° , because the microwave magnetic field component perpendicular to the static magnetic field is proportional to $\cos^2\theta$. The results of this study are presented in Figure 6, for both the low and high field pairs of lines. In this figure, proton hyperfine effects are not illustrated. Each line in this figure represents the average of the doublet. The proton hyperfine effects are illustrated in Figure 7 for the high field doublet.

An isochronal temperature anneal study was done by holding the sample at a desired temperature for 3 minutes and then taking an ESR spectrum at room temperature. Results of this study are shown in Figure 8. At 450K, half of the E'_2 centers have decayed. The initial growth of the E'_2 center is questionable and additional experimental verification will be required.

Two separate programs were written to analyze the experimental data presented in Figure 7. These are listed in Appendices A and B, respectively. The first program, listed in Appendix A, calculates the transition frequencies for a given set of spin Hamiltonian parameters and an assumed magnetic field value. This is equivalent to obtaining data at a fixed value of magnetic field by scanning the microwave frequency. The second program, listed in Appendix B, calculates the final set of parameters (g and A tensors) using the experimental data as in-

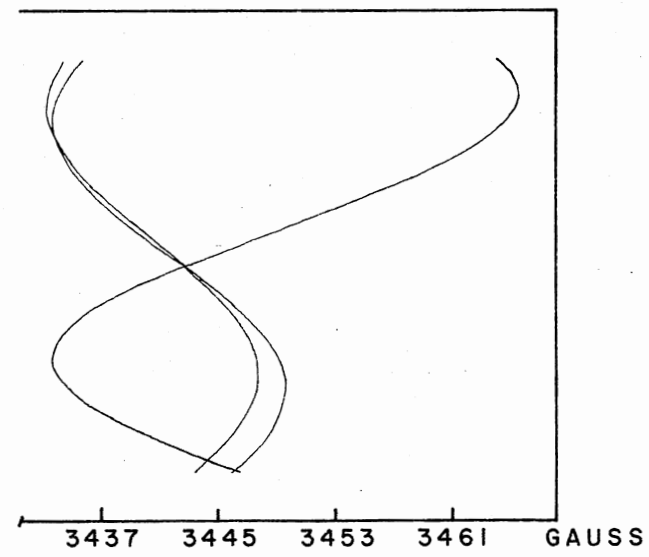
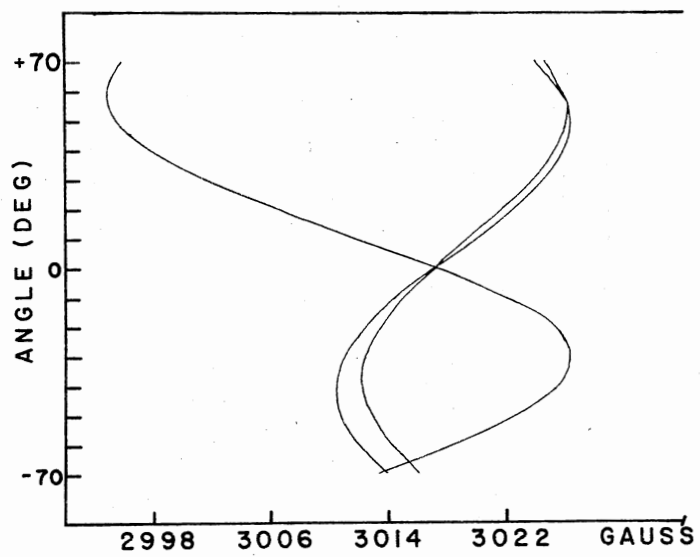


Figure 6. Angular Dependence for ^{29}Si Hyperfine Interaction

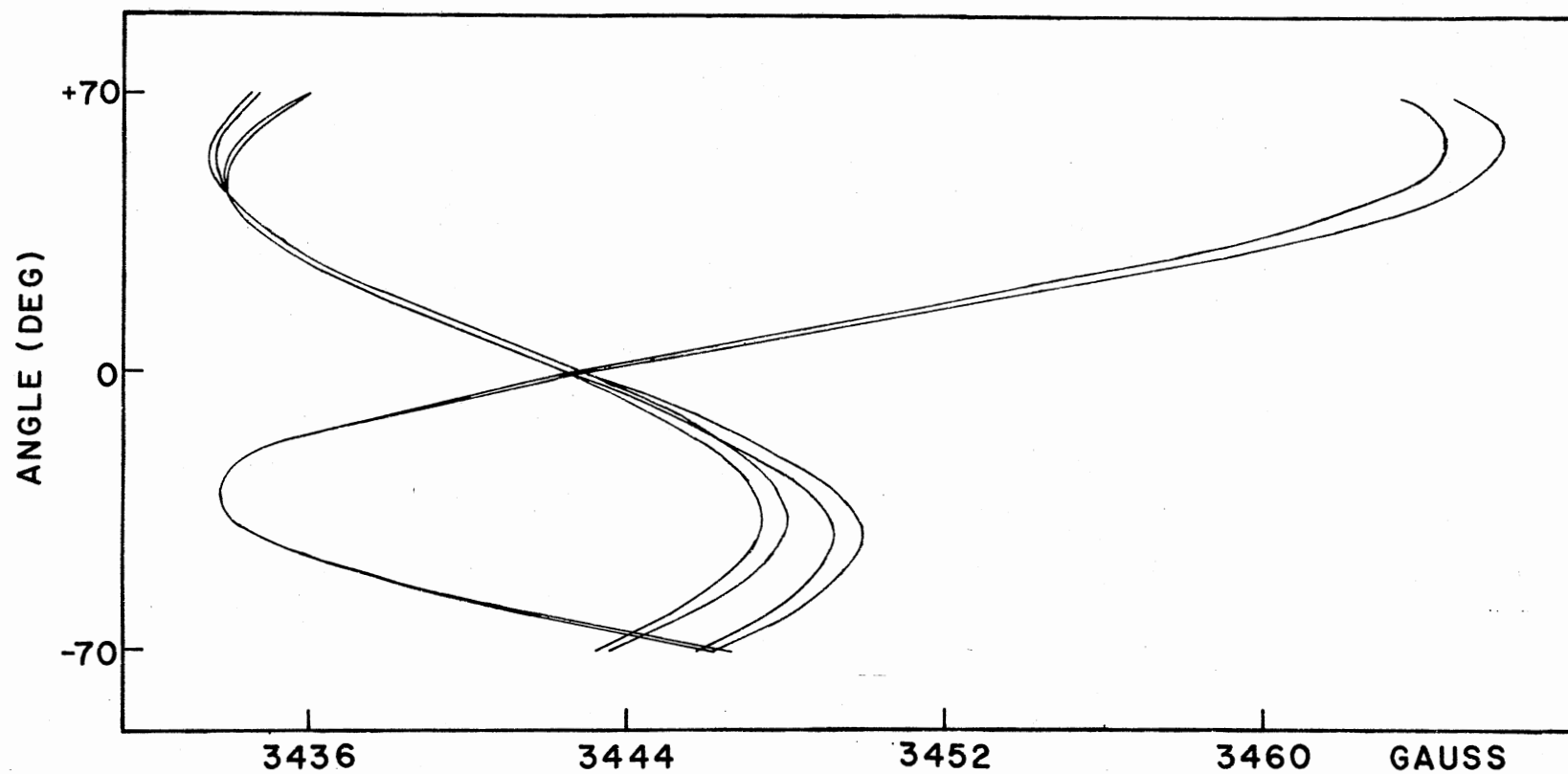


Figure 7. Angular Dependence for the High Field Doublet Illustrating the Proton Effects

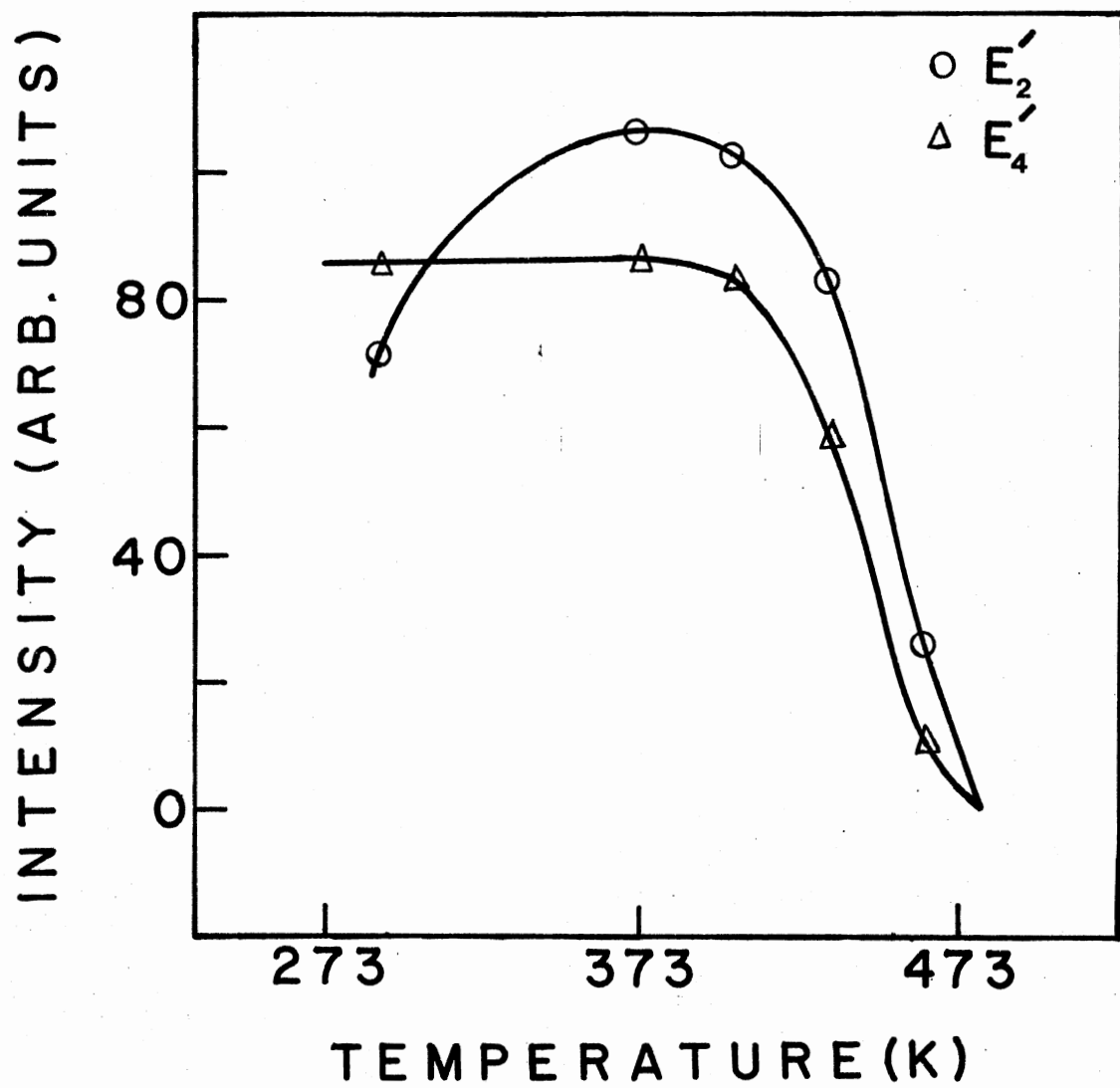


Figure 8. Pulse Anneal Study of the E_2' and the E_4' Center in SiO_2

put.

In the first program, it was assumed that the parameters for the g and A tensors are known. The magnetic field values associated with different ESR resonance lines are predicted by an iteration scheme. An initial value of magnetic field, H , is assigned. The direction of the magnetic field relative to the defect site is specified by the parameters α (α) and β (β). For each set of these angles there are four transitions according to the spin selection rules $\Delta M_s = \pm 1$, $\Delta M_{I_1} = 0$ and $\Delta M_{I_2} = 0$. These possible four transitions are shown in Figure 9. The 8×8 matrix shown in Table I is diagonalized and eight energy eigenvalues $D(I)$ given in order of ascending value are obtained. The four transitions are given by

$$h\nu_1 = D(8) - D(2) ,$$

$$h\nu_2 = D(7) - D(1) ,$$

$$h\nu_3 = D(6) - D(4) ,$$

$$h\nu_4 = D(5) - D(3) .$$

The assigned field value is then varied and the microwave frequency corresponding to a particular transition is recalculated and compared with the experimental microwave frequency 9.085 GHz. If the calculated microwave frequency lies within 0.1 MHz of the experimental frequency, then the microwave frequency for the other, 3 transitions are calculated by iteration.

In the second program, the values of different parameters are systematically varied until a good agreement between the calculated and experimental magnetic field positions is obtained. An initial set of

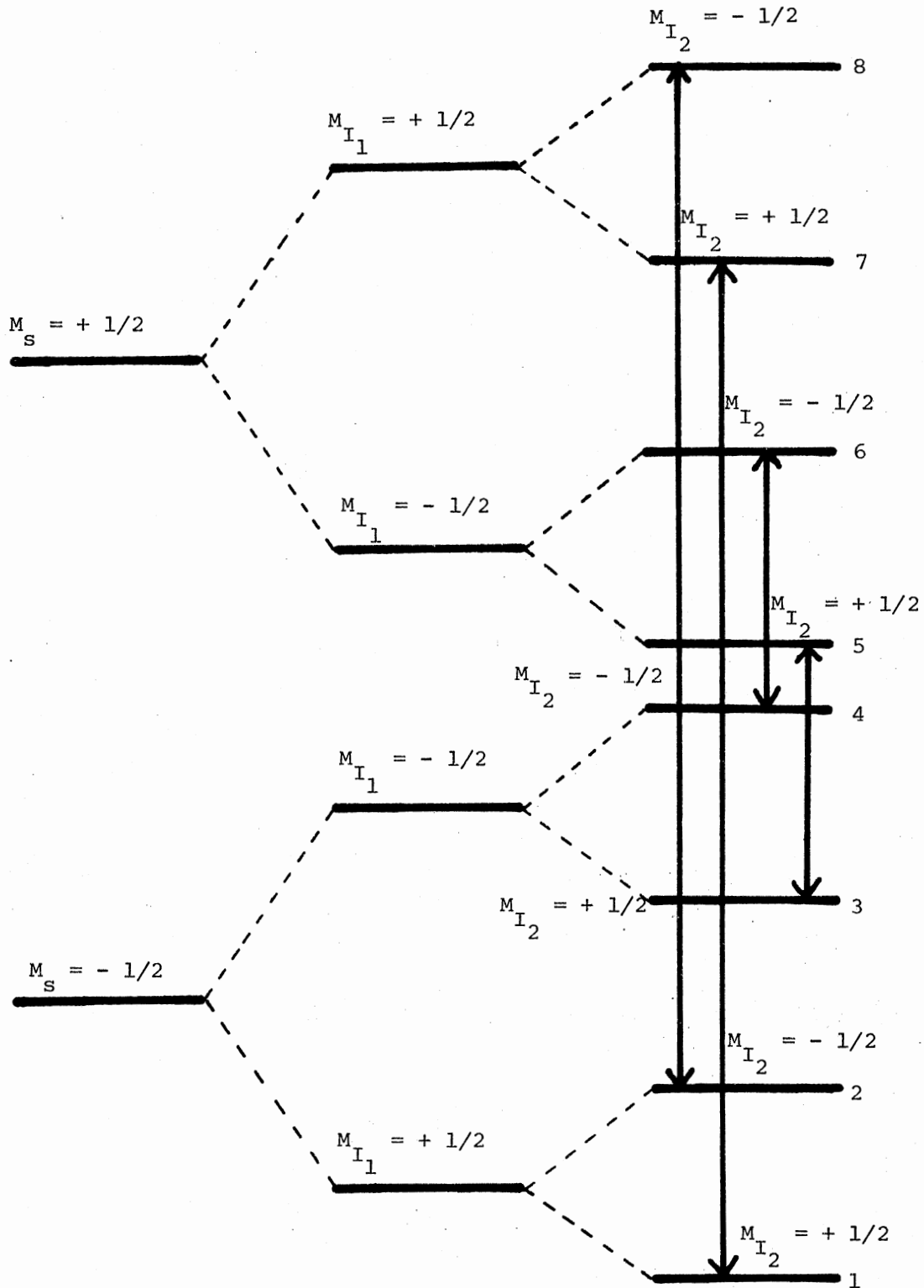


Figure 9. Energy Levels and Possible Transitions in an $S = 1/2$, $I_1 = 1/2$ and $I_2 = 1/2$ System

parameters is assumed and the magnetic field positions for different orientations of the magnetic field are provided as experimental data. Using this information the energy eigenvalues are obtained as in the first program and the microwave frequency associated with each resonance is calculated.

Since the assumed parameters are not the correct ones, the calculated microwave frequency is not the same as the experimental value. Therefore a quantity called SUM

$$\text{SUM} = \sum_{i=1}^{28} [v_i^{\text{exp}} - v_i^{\text{cal}}]^2$$

is calculated. Now the value of SUM is minimized by an iteration technique. Using the assumed set of parameters, the value of SUM is calculated. One of the parameters then is increased by a pre-determined amount and a new set of calculated microwave frequencies are obtained by diagonalization of the matrix. Thus, a new value of SUM is obtained and compared with the previous value of SUM. If the new value of SUM is greater than the previous value, then the value of the parameter (which was increased) is decreased by twice the specified increment. All the microwave frequencies are obtained again and SUM is recalculated. This SUM is compared with the initial value of SUM and the value of the parameter which gives the smallest SUM is retained. This procedure is repeated for all the other parameters.

The final set of parameters was reached when any variation in the parameters failed to lower the value of SUM. The parameters obtained from the computer programs are listed in Table II. The final parameters obtained in this study for the g tensor and proton hyperfine tensor are in good agreement with the parameters listed in Table III

TABLE II

SPIN HAMILTONIAN PARAMETERS FOR THE E_2' CENTER FROM PRESENT STUDY

		z-component	x-component	y-component
Zeeman	g-tensor	2.0020 (120°, 149°)	2.0006 (67°, 73°)	2.0004 (140°, 14°)
H^+	hfs.	4.21 MHz (237°, 26°)	-0.23 MHz (134°, 24°)	-0.56 MHz (117°, -83°)
Si^{29}	hfs.	1312.95 MHz (59°, 27°)	1135.54 MHz (67°, -48°)	1135.51 MHz (140°, -72°)

TABLE III

SPIN HAMILTONIAN PARAMETERS REPORTED BY FEIGEL AND ANDERSON

		z-component	x-component	y-component
Zeeman	g-tensor	2.0020 (120°, 208°)	2.0007 (67°, 133°)	2.0005 (39°, 253°)
H ⁺	hfs.	4.5 MHz (126°, 215°)	-0.3 MHz (44°, 257°)	-0.59 MHz (70°, 140°)
Si ²⁹	Strong hfs.	Not Measured Directly		

which were reported by Feigl and Anderson (8). Discrepancies exist in the angles describing the principal axes directions because of the failure of Feigl and Anderson to choose an appropriate coordinate system. The estimated errors in computing the principal values and directions from this present study are

$$\Delta g = \pm 0.000006$$

$$\Delta A = \pm 0.1 \text{ MHz}$$

$$\Delta \theta = \pm 1^\circ$$

$$\Delta \phi = \pm 1^\circ$$

CHAPTER IV

DISCUSSION

The E'_4 center has been studied in detail recently by L. E. Halliburton and J. A. Weil (10). They have suggested that the E'_4 center is a hydride ion (H^-) sitting in the oxygen vacancy bonding with one silicon with the unpaired electron localized in an sp^3 hybrid orbital on the opposite silicon.

In general, a hyperfine interaction tensor can be separated into two parts--an isotropic part and an anisotropic part with zero trace.

$$\vec{A} = A_0 \vec{1} + \vec{B}$$

The isotropic interaction term (also called the Fermi contact term) is proportional to the probability density of the unpaired electron at the interacting nucleus and is given by

$$A_0 = (8/3) \pi g\beta g_N \beta_N |\psi(\gamma_i)|^2$$

The anisotropic term describes the dipole-dipole interaction of the nuclear magnetic moment with the distributed electronic magnetic moment.

The elements of the B tensor are given by

$$B_{ij} = g\beta g_N \beta_N \int \left[\frac{3x_i x_j}{r^5} - \frac{\delta_{ij}}{r^3} \right] |\psi(\gamma)|^2 d\tau$$

where x_1 , x_2 and x_3 are the Cartesian coordinates of the distributed electronic dipole with respect to the point nuclear dipole.

Now for the E'_2 and the E'_4 center let's assume momentarily that the distributed electronic dipole moment is a point dipole with separation γ from the nuclear magnetic moment along the z axis of the principal coordinate system of the A tensor. From the anisotropic part of the hyperfine tensor A we get

$$\gamma = 1.4 A^0 \quad \text{for the } E'_4 \text{ center}$$

and

$$\gamma = 3.2 A^0 \quad \text{for the } E'_2 \text{ center.}$$

Different γ values for the E'_4 and the E'_2 centers from the simple calculations suggests that these two centers are different in nature. But at the same time we have evidence from our thermal anneal study which suggests that these two centers must be similar in nature. A recent thermal anneal study at low temperatures after various low and high temperature electron irradiation by Mark E. Markes and L. E. Halliburton (11) supports the idea that these two defect centers must be similar in nature. The main question is to find where the proton is sitting in the E'_2 center configuration.

A complete set of experimental data for the ground state of the E'_2 center has now been obtained. But this accumulation of information is insufficient to suggest any concrete model for the E'_2 center. Further theoretical investigations probably will allow one to propose a definite defect model for the E'_2 center in agreement with the experimental data available.

SELECTED BIBLIOGRAPHY

1. Megaw, Helen D. Crystal Structures: A Working Approach (W. B. Saunders Company).
2. Flanagan, T. M. IEEE Transaction on Nuclear Science. NS 21 (1974).
3. Weeks, R. A. and C. M. Nelson. Journal of the American Ceramic Society, 43, 399 (1960).
4. Weeks, R. A. Journal of Applied Physics, 27, 1376 (1956).
5. Silsbee, Robert H. Journal of Applied Physics 32, 1459 (1961).
6. Yip, Kwok Leung and W. B. Fowler, Phys. Rev. B 11, 2327 (1975).
7. Weeks, R. A., Phys. Rev. 130, 570 (1963).
8. Feigl, F. J. and J. H. Anderson, J. Phys. Chem. Solids 31, 575 (1970).
9. Halliburton, L. E. and J. A. Weil, Solid State Commn. (in press).
10. Halliburton, L. E. and J. A. Weil (private communication) (1978).
11. Markes, Mark E. and L. E. Halliburton (private communication) (1979).

APPENDIX A

```

CARD
0001      IMPLICIT REAL * 8 (A-H,O-Z)
0002      REAL * 8 AR(8,8),AI(8,8),E(8),E2(8),TAU(2,8),D(8),HF(8),P(18),
0003      CG(3,3),H(3,3),Z(3,3),RM(3,3),R2(3,3),R3(3,3),RT(3,3),TG(3,3),
0004      CTH(3,3),TZ(3,3),R(3,3),PQ(18)
0005      P(1)=2.0005840+00
0006      P(2)=2.0003780+00
0007      P(3)=2.001710+00
0008      P(4)=120.30+00
0009      P(5)=238.80+00
0010      P(6)=153.20+00
0011      P(7)=1135.540+00
0012      P(8)=1135.510+00
0013      P(9)=1312.950+00
0014      P(10)=58.70+00
0015      P(11)=62.60+00
0016      P(12)=153.20+00
0017      P(13)=-0.2320+00
0018      P(14)=-0.5590+00
0019      P(15)=4.2140+00
0020      P(16)=237.00+00
0021      P(17)=63.50+00
0022      P(18)=56.50+00
0023 C      THE PARAMETERS FOR THE G TENSOR ARE 1-GX, 2-GY, 3-GZ, 4-THETA,
0024 C      5-PHI, 6-PSI. THE PARAMETERS FOR THE HYPERFINE TENSOR ARE 7-AX,
0025 C      8-AY, 9-AZ, 10-THETA, 11-PHI, 12-PSI.
0026 C      THE PARAMETERS FOR PROTON TENSOR ARE 13-A,14-AY,15-AZ,16-THETA,
0027 C      17-PHI,18-PSI.
0028      WRITE(6,10) (P(I),I=1,18)
0029      10 FORMAT(9F10.5)
0030      B=9.27410+00/6.62620+00
0031      GBN1=8.4580-04
0032      GBN2=4.2577080-03
0033      FREQQ=9.0850+03
0034      N=8
0035      NM=8
0036      ALPHA= 0.00+00
0037      BETA= -9.00+01
0038      DO 91 L=1,3
0039      P(L+3)=P(L+3)*(3.141590+00/1.80+02)
0040      P(L+9)=P(L+9)*(3.141590+00/1.80+02)
0041      91 P(L+15)=P(L+15)*(3.141590+00/1.80+02)
0042      AG=OSIN(P(4))
0043      AAG=OCOS(P(4))
0044      CG=OSIN(P(5))
0045      CCG=OCOS(P(5))
0046      FG=OSIN(P(6))
0047      FFG=OCOS(P(6))
0048      AH=OSIN(P(10))
0049      AAH=OCOS(P(10))
0050      CH=OSIN(P(11))
0051      CCH=OCOS(P(11))
0052      FH=OSIN(P(12))
0053      FFH=OCOS(P(12))
0054      AZ=OSIN(P(16))
0055      AAZ=OCOS(P(16))
0056      CZ=OSIN(P(17))
0057      CCZ=OCOS(P(17))
0058      FZ=OSIN(P(18))
0059      FFZ=OCOS(P(18))
0060      CO=OCOS(2.0943950+00)
0061      SI=OSIN(2.0943950+00)
0062      G(1,1)=FFG*CCG-AAG*CG*FG
0063      G(1,2)=FFG*CG+AAG*CCG*FG
0064      G(1,3)=FG*AG
0065      G(2,1)=-FG*CCG-AAG*CG*FFG
0066      G(2,2)=-FG*CG+AAG*CCG*FFG
0067      G(2,3)=FFG*AG
0068      G(3,1)=AG*CG

```

```

0069      G(3,2)=-AG*CCG
0070      G(3,3)=AAG
0071      H(1,1)=FFH*CCH-AAH*CH*FH
0072      H(1,2)=FFH*CH+AAH*CCH*FH
0073      H(1,3)=FH*AH
0074      H(2,1)=-FH*CCH-AAH*CH*FFH
0075      H(2,2)=-FH*CH+AAH*CCH*FFH
0076      H(2,3)=FFH*AH
0077      H(3,1)=AH*CH
0078      H(3,2)=-AH*CCH
0079      H(3,3)=AAH
0080      Z(1,1)=FFZ*CCZ-AAZ*CZ*FZ
0081      Z(1,2)=FFZ*CZ+AAZ*CCZ*FZ
0082      Z(1,3)=FZ*AZ
0083      Z(2,1)=-FZ*CCZ-AAZ*CZ*FFZ
0084      Z(2,2)=-FZ*CZ+AAZ*CCZ*FFZ
0085      Z(2,3)=FFZ*AZ
0086      Z(3,1)=AZ*CZ
0087      Z(3,2)=-AZ*CCZ
0088      Z(3,3)=AAZ
0089      20 ALPHAR=ALPHA*(3.141590+00/1.80+02)
0090      BETAR=BET A*(3.141590+00/1.80+02)
0091      WRITE(6,30) ALPHA, BETA
0092      30 FORMAT('0',2F15.3)
0093      RM(1,1)=DCOS(ALPHAR)
0094      RM(1,2)=-DSIN(ALPHAR)*DSIN(BETAR)
0095      RM(1,3)=DSIN(ALPHAR)*DCOS(BETAR)
0096      RM(2,1)=0.00+00
0097      RM(2,2)=DCOS(BETAR)
0098      RM(2,3)=DSIN(BETAR)
0099      RM(3,1)=-DSIN(ALPHAR)
0100      RM(3,2)=-DCOS(ALPHAR)*DSIN(BETAR)
0101      RM(3,3)=DCOS(ALPHAR)*DCOS(BETAR)
0102      K = 1
0103      40 GO TO (50,50,50,60,60,60),K
0104      50 R2(1,1)=1.00+00
0105      R2(1,2)=0.00+00
0106      R2(1,3)=0.00+00
0107      R2(2,1)=0.00+00
0108      R2(2,2)=1.00+00
0109      R2(2,3)=0.00+00
0110      R2(3,1)=0.00+00
0111      R2(3,2)=0.00+00
0112      R2(3,3)=1.00+00
0113      GO TO (70,80,90),K
0114      60 R2(1,1)=1.00+00
0115      R2(1,2)=0.00+00
0116      R2(1,3)=0.00+00
0117      R2(2,1)=0.00+00
0118      R2(2,2)=-1.00+00
0119      R2(2,3)=0.00+00
0120      R2(3,1)=0.00+00
0121      R2(3,2)=0.00+00
0122      R2(3,3)=-1.00+00
0123      KK = K-3
0124      GO TO (70,80,90),KK
0125      70 R3(1,1)=1.00+00
0126      R3(1,2)=0.00+00
0127      R3(1,3)=0.00+00
0128      R3(2,1)=0.00+00
0129      R3(2,2)=1.00+00
0130      R3(2,3)=0.00+00
0131      R3(3,1)=0.00+00
0132      R3(3,2)=0.00+00
0133      R3(3,3)=1.00+00
0134      GO TO 100
0135      80 R3(1,1)=CO
0136      R3(1,2)=SI
0137      R3(1,3)=0.00+00
0138      R3(2,1)=-SI

```

```

0139      R3(2,2)=C0
0140      R3(2,3)=0.00+00
0141      R3(3,1)=0.00+00
0142      R3(3,2)=0.00+00
0143      R3(3,3)=1.00+00
0144      GO TO 100
0145  90  R3(1,1)=C0
0146      R3(1,2)=-S1
0147      R3(1,3)=0.00+00
0148      R3(2,1)=S1
0149      R3(2,2)=C0
0150      R3(2,3)=0.00+00
0151      R3(3,1)=0.00+00
0152      R3(3,2)=0.00+00
0153      R3(3,3)=1.00+00
0154  100 DO 110 L=1,3
0155      DO 110 M=1,3
0156  110 RT(L,M)=R2(L,1)*R3(1,M)+R2(L,2)*R3(2,M)+R2(L,3)*R3(3,M)
0157      DO 120 L=1,3
0158      DO 120 M=1,3
0159  120 R(L,M)=RT(L,1)*RM(1,M)+RT(L,2)*RM(2,M)+RT(L,3)*RM(3,M)
0160      DO 130 L=1,3
0161      DO 130 M=1,3
0162      TG(L,M)=G(L,1)*R(1,M)+G(L,2)*R(2,M)+G(L,3)*R(3,M)
0163      TH(L,M)=H(L,1)*R(1,M)+H(L,2)*R(2,M)+H(L,3)*R(3,M)
0164  130 TZ(L,M)=Z(L,1)*R(1,M)+Z(L,2)*R(2,M)+Z(L,3)*R(3,M)
0165      I=1
0166  140 HH=6.000+03
0167  150 W1=8*HH*(P(1)*TG(1,1)*TG(1,3)+P(2)*TG(2,1)*TG(2,3)+P(3)*TG(3,1)*
0168      CTG(3,3))
0169      W2=8*HH*(P(1)*TG(1,2)*TG(1,3)+P(2)*TG(2,2)*TG(2,3)+P(3)*TG(3,2)*
0170      CTG(3,3))
0171      W3=8*HH*(P(1)*TG(1,3)*TG(1,3)+P(2)*TG(2,3)*TG(2,3)+P(3)*TG(3,3)*
0172      CTG(3,3))
0173      W4=P(7)*TH(1,1)*TH(1,1)+P(8)*TH(2,1)*TH(2,1)+P(9)*TH(3,1)*TH(3,1)
0174      W5=P(7)*TH(1,1)*TH(1,2)+P(8)*TH(2,1)*TH(2,2)+P(9)*TH(3,1)*TH(3,2)
0175      W6=P(7)*TH(1,1)*TH(1,3)+P(8)*TH(2,1)*TH(2,3)+P(9)*TH(3,1)*TH(3,3)
0176      W7=P(7)*TH(1,2)*TH(1,2)+P(8)*TH(2,2)*TH(2,2)+P(9)*TH(3,2)*TH(3,2)
0177      W8=P(7)*TH(1,2)*TH(1,3)+P(8)*TH(2,2)*TH(2,3)+P(9)*TH(3,2)*TH(3,3)
0178      W9=P(7)*TH(1,3)*TH(1,3)+P(8)*TH(2,3)*TH(2,3)+P(9)*TH(3,3)*TH(3,3)
0179      W10=P(13)*TZ(1,1)*TZ(1,1)+P(14)*TZ(2,1)*TZ(2,1)+P(15)*TZ(3,1)
0180      C*TZ(3,1)
0181      W11=P(13)*TZ(1,1)*TZ(1,2)+P(14)*TZ(2,1)*TZ(2,2)+P(15)*TZ(3,1)
0182      C*TZ(3,2)
0183      W12=P(13)*TZ(1,1)*TZ(1,3)+P(14)*TZ(2,1)*TZ(2,3)+P(15)*TZ(3,1)
0184      C*TZ(3,3)
0185      W13=P(13)*TZ(1,2)*TZ(1,2)+P(14)*TZ(2,2)*TZ(2,2)+P(15)*TZ(3,2)
0186      C*TZ(3,2)
0187      W14=P(13)*TZ(1,2)*TZ(1,3)+P(14)*TZ(2,2)*TZ(2,3)+P(15)*TZ(3,2)
0188      C*TZ(3,3)
0189      W15=P(13)*TZ(1,3)*TZ(1,3)+P(14)*TZ(2,3)*TZ(2,3)+P(15)*TZ(3,3)
0190      C*TZ(3,3)
0191      Q1R=W1/2.00+00
0192      Q1I= W2/2.00+00
0193      Q2R= (W4-W7)/4.00+00
0194      Q2I= W5/2.00+00
0195      Q3= (W4+W7)/4.00+00
0196      Q4R= W6/2.00+00
0197      Q4I= W8/2.00+00
0198      Q5R=(W10-W13)/4.00+00
0199      Q5I=W11/2.00+00
0200      Q6=(W10+W13)/4.00+00
0201      Q7R=W12/2.00+00
0202      Q7I=W14/2.00+00
0203      DO 160 L=1,8
0204      DO 160 M=1,8
0205      AR(L,M)= 0.00+00
0206  160 AI(L,M)= 0.00+00
0207      AR(1,1)=W3/2.00+00+W9/4.00+00+W15/4.00+00-(GBN1*HH)/2.00+00
0208      C-(GBN2*HH)/2.00+00

```

```

0209      AR(2,2)=W3/2.0D+00-W9/4.0D+00+W15/4.0D+00+(GBN1*HH)/2.0D+00
0210      C-(GBN2*HH)/2.0D+00
0211      AR(3,3)=-W3/2.0D+00-W9/4.0D+00-W15/4.0D+00-(GBN1*HH)/2.0D+00
0212      C-(GBN2*HH)/2.0D+00
0213      AR(4,4)=-W3/2.0D+00+W9/4.0D+00-W15/4.0D+00+(GBN1*HH)/2.0D+00
0214      C-(GBN2*HH)/2.0D+00
0215      AR(5,5)=W3/2.0D+00+W9/4.0D+00-W15/4.0D+00-(GBN1*HH)/2.0D+00
0216      C+(GBN2*HH)/2.0D+00
0217      AR(6,6)=W3/2.0D+00-W9/4.0D+00-W15/4.0D+00+(GBN1*HH)/2.0D+00
0218      C+(GBN2*HH)/2.0D+00
0219      AR(7,7)=-W3/2.0D+00-W9/4.0D+00+W15/4.0D+00-(GBN1*HH)/2.0D+00
0220      C+(GBN2*HH)/2.0D+00
0221      AR(8,8)=-W3/2.0D+00+W9/4.0D+00+W15/4.0D+00+(GBN1*HH)/2.0D+00
0222      C+(GBN2*HH)/2.0D+00
0223      AR(2,1)=Q4R/2.0D+00
0224      AI(2,1)=Q4I/2.0D+00
0225      AR(3,1)=Q1R+Q4R/2.0D+00+Q7R/2.0D+00
0226      AI(3,1)=Q1I+Q4I/2.0D+00+Q7I/2.0D+00
0227      AR(4,1)=Q2R
0228      AI(4,1)=Q2I
0229      AR(5,1)=Q7R/2.0D+00
0230      AI(5,1)=Q7I/2.0D+00
0231      AR(7,1)=Q5R
0232      AI(7,1)=Q5I
0233      AR(3,2)=Q3
0234      AR(4,2)=Q1R-Q4R/2.0D+00+Q7R/2.0D+00
0235      AI(4,2)=Q1I-Q4I/2.0D+00+Q7I/2.0D+00
0236      AR(6,2)=AR(5,1)
0237      AI(6,2)=AI(5,1)
0238      AR(8,2)=AR(7,1)
0239      AI(8,2)=AI(7,1)
0240      AR(4,3)=-AR(2,1)
0241      AI(4,3)=-AI(2,1)
0242      AR(5,3)=Q6
0243      AR(7,3)=-AR(5,1)
0244      AI(7,3)=-AI(5,1)
0245      AR(6,4)=AR(5,3)
0246      AR(8,4)=AR(7,3)
0247      AI(8,4)=AI(7,3)
0248      AR(6,5)=-AR(4,3)
0249      AI(6,5)=-AI(4,3)
0250      AR(7,5)=Q1R+Q4R/2.0D+00-Q7R/2.0D+00
0251      AI(7,5)=Q1I+Q4I/2.0D+00-Q7I/2.0D+00
0252      AR(8,5)=AR(4,1)
0253      AI(8,5)=AI(4,1)
0254      AR(7,6)=AR(3,2)
0255      AR(8,6)=Q1R-Q4R/2.0D+00-Q7R/2.0D+00
0256      AI(8,6)=Q1I-Q4I/2.0D+00-Q7I/2.0D+00
0257      AR(8,7)=-Q4R/2.0D+00
0258      AI(8,7)=-Q4I/2.0D+00
0259      CALL HTRIDI (NM,N,AR,AI,D,E,E2,TAU)
0260      CALL IMTQL1 (N,D,E,IERR)
0261      GO TO (170,180,190,200),I
0262      170  FREQ=D(8)-D(2)
0263      GO TO 210
0264      180  FREQ=D(7)-D(1)
0265      GO TO 210
0266      190  FREQ=D(6)-D(4)
0267      GO TO 210
0268      200  FREQ=D(5)-D(3)
0269      210  IF(DABS(FREQQ-FREQ)-1.0D-01)220,220,230
0270      220  HF(I)=HH
0271      GO TO 240
0272      230  HH=HH*(FREQQ/FREQ)
0273      GO TO 150
0274      240  IF(I-4)250,260,260
0275      250  I=I+1
0276      GO TO 140
0277      260  WRITE(6,270) (HF(I),I=1,4)
0278      270  FORMAT(4F20.2)

```

```
0279      IF(K-6)280,290,290
0280 280 K=K+1
0281      GO TO 40
0282 290 BETA=BETA+5.00+00
0283      IF(BETA-9.10+01)20,300,300
0284 300 WRITE(6,310) (P(I),I=1,19)
0285 310 FORMAT('0',9F10.5)
0286      PQ(1)=DARCOS(G(1,3))
0287      PQ(2)=DATAN(G(1,2)/G(1,1))
0288      PQ(3)=DARCOS(G(2,3))
0289      PQ(4)=DATAN(G(2,2)/G(2,1))
0290      PQ(5)=P(4)
0291      PQ(6)=DARCOS(CG)
0292      PQ(7)=DARCOS(H(1,3))
0293      PQ(8)=DATAN(H(1,2)/H(1,1))
0294      PQ(9)=DARCOS(H(2,3))
0295      PQ(10)=DATAN(H(2,2)/H(2,1))
0296      PQ(11)=P(10)
0297      PQ(12)=DARCOS(CH)
0298      PQ(13)=DARCOS(Z(1,3))
0299      PQ(14)=DATAN(Z(1,2)/Z(1,1))
0300      PQ(15)=DARCOS(Z(2,3))
0301      PQ(16)=DATAN(Z(2,2)/Z(2,1))
0302      PQ(17)=P(16)
0303      PQ(18)=DARCOS(CZ)
0304      DO 320 L=1,18
0305 320 PQ(L)=PQ(L)*(1.80+02/3.141590+00)
0306      WRITE(6,330) (PQ(I),I=1,18)
0307 330 FORMAT('0',6F15.5)
0308      STOP
0309      END
```

APPENDIX B


```

CAPD
0001      IMPLICIT REAL * 8 (A-H,O-Z)
0002      REAL * 8 AR(8,8),AI(8,8),E(8),E2(8),TAU(2,8),D(8),HF(8),P(13),
0003      CG(3,3),H(3,3),Z(3,3),RM(3,3),R2(3,3),R3(3,3),RT(3,3),TG(3,3),
0004      CTH(3,3),TZ(3,3),R(3,3),FREQ1(28)
0005      P(1)=2.000584D+00
0006      P(2)=2.000378D+00
0007      P(3)=2.00171D+00
0008      P(4)=120.3D+00
0009      P(5)=238.8D+00
0010      P(6)=153.2D+00
0011      P(7)=1135.54D+00
0012      P(8)=1135.51D+00
0013      P(9)=1312.95D+00
0014      P(10)=58.7D+00
0015      P(11)=62.6D+00
0016      P(12)=153.2D+00
0017      P(13)=-0.232D+00
0018      P(14)=-0.559D+00
0019      P(15)=4.214D+00
0020      P(16)=237.0D+00
0021      P(17)=63.5D+00
0022      P(18)=56.5D+00
0023      C   THE PARAMETERS FOR THE G TENSOR ARE 1-GX, 2-GY, 3-GZ, 4-THETA,
0024      C   5-PHI, 6-PSI. THE PARAMETERS FOR THE HYPERFINE TENSOR ARE 7-AX,
0025      C   8-AY, 9-AZ, 10-THETA, 11-PHI, 12-PSI.
0026      C   THE PARAMETERS FOR PROTON TENSOR ARE 13-A,14-AY,15-AZ,16-THETA,
0027      C   17-PHI,18-PSI.
0028      WRITE(6,10) (P(I),I=1,18)
0029      10  FORMAT('0',6F10.5)
0030      B=9.2741D+00/6.6262D+00
0031      GBN1=8.458D-04
0032      GBN2=4.2577D-03
0033      FREQQ=9.085D+03
0034      N=8
0035      NM=8
0036      ALPHA= 0.0D+00
0037      DO 91 L=1,3
0038      P(L+3)=P(L+3)*(3.14159D+00/1.8D+02)
0039      P(L+9)=P(L+9)*(3.14159D+00/1.8D+02)
0040      91  P(L+15)=P(L+15)*(3.14159D+00/1.8D+02)
0041      92  DO 93 LL=13,18
0042      94  K1=1
0043      95  MM=1
0044      96  GO TO (358,359,360,361,362,363,364,365,366,367,368,369,370,
0045      C371,372,373,374,375,376,377,378,379,380,381,382,383,384,385),MM
0046      358  HH=2996.655D+00
0047      BETA=70.0D+00
0048      K=2
0049      I=1
0050      GO TO 97
0051      359  HH=3434.567D+00
0052      K=1
0053      I=3
0054      GO TO 97
0055      360  HH=3435.957D+00
0056      K=3
0057      I=4
0058      GO TO 97
0059      361  HH=2995.592D+00
0060      BETA=60.0D+00
0061      K=2
0062      I=1
0063      GO TO 97
0064      362  HH=3433.756D+00
0065      K=1
0066      I=4
0067      GO TO 97
0068      363  HH=2997.236D+00

```

0069 BETA=45.00+00
0070 K=2
0071 I=1
0072 GO TO 97
0073 364 HH=2995.7760+00
0074 I=2
0075 365 HH=3025.920+00
0076 K=1
0077 I=2
0078 GO TO 97
0079 366 HH=3026.2750+00
0080 K=3
0081 GO TO 97
0082 367 HH=3002.3030+00
0083 BETA=30.00+00
0084 K=2
0085 I=1
0086 GO TO 97
0087 368 HH=3024.0280+00
0088 K=1
0089 I=1
0090 GO TO 97
0091 369 HH=3024.70350+00
0092 K=3
0093 GO TO 97
0094 370 HH=3009.7120+00
0095 BETA=15.00+00
0096 K=2
0097 I=1
0098 GO TO 97
0099 371 HH=3020.90+00
0100 K=1
0101 I=1
0102 GO TO 97
0103 372 HH=3021.4110+00
0104 K=3
0105 GO TO 97
0106 373 HH=3017.5230+00
0107 BETA=0.00+00
0108 K=2
0109 I=1
0110 GO TO 97
0111 374 HH=3023.6420+00
0112 BETA=-15.00+00
0113 K=2
0114 I=1
0115 GO TO 97
0116 375 HH=3026.2770+00
0117 BETA=-30.00+00
0118 K=2
0119 I=1
0120 GO TO 97
0121 376 HH=3011.4670+00
0122 K=3
0123 I=1
0124 GO TO 97
0125 377 HH=3012.850+00
0126 K=1
0127 I=1
0128 GO TO 97
0129 378 HH=3024.3870+00
0130 BETA=-45.00+00
0131 K=2
0132 I=1
0133 GO TO 97
0134 379 HH=3012.810+00
0135 K=1
0136 I=1
0137 GO TO 97
0138 380 HH=3010.9030+00

```

0139      K=3
0140      I=1
0141      GO TO 97
0142 381 HH=3018.6680+00
0143      BETA=-60.00+00
0144      K=2
0145      I=1
0146      GO TO 97
0147 382 HH=3014.4510+00
0148      K=1
0149      I=1
0150      GO TO 97
0151 383 HH=3012.3080+00
0152      K=3
0153      I=1
0154      GO TO 97
0155 384 HH=3014.2110+00
0156      BETA=-70.00+00
0157      K=3
0158      I=1
0159      GO TO 97
0160 385 HH=3445.7870+00
0161      K=3
0162      I=4
0163 97 AG=OSIN(P(4))
0164      AAG=OCOS(P(4))
0165      CG=OSIN(P(5))
0166      CCG=OCOS(P(5))
0167      FG=OSIN(P(6))
0168      FFG=OCOS(P(6))
0169      AH=OSIN(P(10))
0170      AAH=OCOS(P(10))
0171      CH=OSIN(P(11))
0172      CCH=OCOS(P(11))
0173      FH=OSIN(P(12))
0174      FFH=OCOS(P(12))
0175      AZ=OSIN(P(16))
0176      AAZ=OCOS(P(16))
0177      CZ=OSIN(P(17))
0178      CCZ=OCOS(P(17))
0179      FZ=OSIN(P(18))
0180      FFZ=OCOS(P(18))
0181      CO=OCOS(2.0943950+00)
0182      SI=OSIN(2.0943950+00)
0183      G(1,1)=FFG*CCG-AAG*CG*FG
0184      G(1,2)=FFG*CG+AAG*CCG*FFG
0185      G(1,3)=FG*AG
0186      G(2,1)=-FG*CCG-AAG*CG*FFG
0187      G(2,2)=-FG*CG+AAG*CCG*FFG
0188      G(2,3)=FFG*AG
0189      G(3,1)=AG*CG
0190      G(3,2)=-AG*CCG
0191      G(3,3)=AAG
0192      H(1,1)=FFH*CCH-AAH*CH*FH
0193      H(1,2)=FFH*CH+AAH*CCH*FH
0194      H(1,3)=FH*AH
0195      H(2,1)=-FH*CCH-AAH*CH*FFH
0196      H(2,2)=-FH*CH+AAH*CCH*FFH
0197      H(2,3)=FFH*AH
0198      H(3,1)=AH*CH
0199      H(3,2)=-AH*CCH
0200      H(3,3)=AAH
0201      Z(1,1)=FFZ*CCZ-AAZ*CZ*FZ
0202      Z(1,2)=FFZ*CZ+AAZ*CCZ*FZ
0203      Z(1,3)=FZ*AZ
0204      Z(2,1)=-FZ*CCZ-AAZ*CZ*FFZ
0205      Z(2,2)=-FZ*CZ+AAZ*CCZ*FFZ
0206      Z(2,3)=FFZ*AZ
0207      Z(3,1)=AZ*CZ
0208      Z(3,2)=-AZ*CCZ

```

```

0209     Z(3,3)=AAZ
0210     20 ALPHAR=ALPHA*(3.14159D+00/1.8D+02)
0211     BETAR=BETA*(3.14159D+00/1.8D+02)
0212     RM(1,1)=DCOS(ALPHAR)
0213     RM(1,2)=-DSIN(ALPHAR)*DSIN(BETAR)
0214     RM(1,3)=DSIN(ALPHAR)*DCOS(BETAR)
0215     RM(2,1)=0.0D+00
0216     RM(2,2)=DCOS(BETAR)
0217     RM(2,3)=DSIN(BETAR)
0218     RM(3,1)=-DSIN(ALPHAR)
0219     RM(3,2)=-DCOS(ALPHAR)*DSIN(BETAR)
0220     RM(3,3)=DCOS(ALPHAR)*DCOS(BETAR)
0221     40 GO TO (50,50,50,60,60,60),K
0222     50 R2(1,1)=1.0D+00
0223     R2(1,2)=0.0D+00
0224     R2(1,3)=0.0D+00
0225     R2(2,1)=0.0D+00
0226     R2(2,2)=1.0D+00
0227     R2(2,3)=0.0D+00
0228     R2(3,1)=0.0D+00
0229     R2(3,2)=0.0D+00
0230     R2(3,3)=1.0D+00
0231     GO TO (70,80,90),K
0232     60 R2(1,1)=1.0D+00
0233     R2(1,2)=0.0D+00
0234     R2(1,3)=0.0D+00
0235     R2(2,1)=0.0D+00
0236     R2(2,2)=-1.0D+00
0237     R2(2,3)=0.0D+00
0238     R2(3,1)=0.0D+00
0239     R2(3,2)=0.0D+00
0240     R2(3,3)=-1.0D+00
0241     KK = K-3
0242     GO TO (70,80,90),KK
0243     70 R3(1,1)=1.0D+00
0244     R3(1,2)=0.0D+00
0245     R3(1,3)=0.0D+00
0246     R3(2,1)=0.0D+00
0247     R3(2,2)=1.0D+00
0248     R3(2,3)=0.0D+00
0249     R3(3,1)=0.0D+00
0250     R3(3,2)=0.0D+00
0251     R3(3,3)=1.0D+00
0252     GO TO 100
0253     80 R3(1,1)=CO
0254     R3(1,2)=SI
0255     R3(1,3)=0.0D+00
0256     R3(2,1)=-SI
0257     R3(2,2)=CO
0258     R3(2,3)=0.0D+00
0259     R3(3,1)=0.0D+00
0260     R3(3,2)=0.0D+00
0261     R3(3,3)=1.0D+00
0262     GO TO 100
0263     90 R3(1,1)=CO
0264     R3(1,2)=-SI
0265     R3(1,3)=0.0D+00
0266     R3(2,1)=SI
0267     R3(2,2)=CO
0268     R3(2,3)=0.0D+00
0269     R3(3,1)=0.0D+00
0270     R3(3,2)=0.0D+00
0271     R3(3,3)=1.0D+00
0272     100 DO 110 L=1,3
0273     DO 110 M=1,3
0274     110 RT(L,M)=R2(L,1)*R3(1,M)+R2(L,2)*R3(2,M)+R2(L,3)*R3(3,M)
0275     DO 120 L=1,3
0276     DO 120 M=1,3
0277     120 R(L,M)=RT(L,1)*RM(1,M)+RT(L,2)*RM(2,M)+RT(L,3)*RM(3,M)
0278     DO 130 L=1,3

```

```

0279      DD 130 M=1,3
0280      TG(L,M)=G(L,1)*R(1,M)+G(L,2)*R(2,M)+G(L,3)*R(3,M)
0281      TH(L,M)=H(L,1)*R(1,M)+H(L,2)*R(2,M)+H(L,3)*R(3,M)
0282      TZ(L,M)=Z(L,1)*R(1,M)+Z(L,2)*R(2,M)+Z(L,3)*R(3,M)
0283      130 W1=8*HH*(P(1)*TG(1,1)*TG(1,3)+P(2)*TG(2,1)*TG(2,3)+P(3)*TG(3,1)*
0284      CTG(3,3))
0285      W2=8*HH*(P(1)*TG(1,2)*TG(1,3)+P(2)*TG(2,2)*TG(2,3)+P(3)*TG(3,2)*
0286      CTG(3,3))
0287      W3=8*HH*(P(1)*TG(1,3)*TG(1,3)+P(2)*TG(2,3)*TG(2,3)+P(3)*TG(3,3)*
0288      CTG(3,3))
0289      W4=P(7)*TH(1,1)*TH(1,1)+P(8)*TH(2,1)*TH(2,1)+P(9)*TH(3,1)*TH(3,1)
0290      W5=P(7)*TH(1,1)*TH(1,2)+P(8)*TH(2,1)*TH(2,2)+P(9)*TH(3,1)*TH(3,2)
0291      W6=P(7)*TH(1,1)*TH(1,3)+P(8)*TH(2,1)*TH(2,3)+P(9)*TH(3,1)*TH(3,3)
0292      W7=P(7)*TH(1,2)*TH(1,2)+P(8)*TH(2,2)*TH(2,2)+P(9)*TH(3,2)*TH(3,2)
0293      W8=P(7)*TH(1,2)*TH(1,3)+P(8)*TH(2,2)*TH(2,3)+P(9)*TH(3,2)*TH(3,3)
0294      W9=P(7)*TH(1,3)*TH(1,3)+P(8)*TH(2,3)*TH(2,3)+P(9)*TH(3,3)*TH(3,3)
0295      W10=P(13)*TZ(1,1)*TZ(1,1)+P(14)*TZ(2,1)*TZ(2,1)+P(15)*TZ(3,1)
0296      C*TZ(3,1))
0297      W11=P(13)*TZ(1,1)*TZ(1,2)+P(14)*TZ(2,1)*TZ(2,2)+P(15)*TZ(3,1)
0298      C*TZ(3,2))
0299      W12=P(13)*TZ(1,1)*TZ(1,3)+P(14)*TZ(2,1)*TZ(2,3)+P(15)*TZ(3,1)
0300      C*TZ(3,3))
0301      W13=P(13)*TZ(1,2)*TZ(1,2)+P(14)*TZ(2,2)*TZ(2,2)+P(15)*TZ(3,2)
0302      C*TZ(3,2))
0303      W14=P(13)*TZ(1,2)*TZ(1,3)+P(14)*TZ(2,2)*TZ(2,3)+P(15)*TZ(3,2)
0304      C*TZ(3,3))
0305      W15=P(13)*TZ(1,3)*TZ(1,3)+P(14)*TZ(2,3)*TZ(2,3)+P(15)*TZ(3,3)
0306      C*TZ(3,3))
0307      Q1R=W1/2.00+00
0308      Q1I= W2/2.00+00
0309      Q2R= (W4-W7)/4.00+00
0310      Q2I= W5/2.00+00
0311      Q3= (W4+W7)/4.00+00
0312      Q4R= W6/2.00+00
0313      Q4I= W8/2.00+00
0314      Q5R=(W10-W13)/4.00+00
0315      Q5I=W11/2.00+00
0316      Q6=(W10+W13)/4.00+00
0317      Q7R=W12/2.00+00
0318      Q7I=W14/2.00+00
0319      DD 160 L=1,8
0320      DD 160 M=1,8
0321      AR(L,M)= 0.00+00
0322      160 AI(L,M)= 0.00+00
0323      AR(1,1)=W3/2.00+00+W9/4.00+00+W15/4.00+00-(GBN1*HH)/2.00+00
0324      C-(GBN2*HH)/2.00+00
0325      AR(2,2)=W3/2.00+00-W9/4.00+00+W15/4.00+00+(GBN1*HH)/2.00+00
0326      C-(GBN2*HH)/2.00+00
0327      AR(3,3)=-W3/2.00+00-W9/4.00+00-W15/4.00+00-(GBN1*HH)/2.00+00
0328      C-(GBN2*HH)/2.00+00
0329      AR(4,4)=-W3/2.00+00+W9/4.00+00-W15/4.00+00+(GBN1*HH)/2.00+00
0330      C-(GBN2*HH)/2.00+00
0331      AR(5,5)=W3/2.00+00+W9/4.00+00-W15/4.00+00-(GBN1*HH)/2.00+00
0332      C+(GBN2*HH)/2.00+00
0333      AR(6,6)=W3/2.00+00-W9/4.00+00-W15/4.00+00+(GBN1*HH)/2.00+00
0334      C+(GBN2*HH)/2.00+00
0335      AR(7,7)=-W3/2.00+00-W9/4.00+00+W15/4.00+00-(GBN1*HH)/2.00+00
0336      C+(GBN2*HH)/2.00+00
0337      AR(8,8)=-W3/2.00+00+W9/4.00+00+W15/4.00+00+(GBN1*HH)/2.00+00
0338      C+(GBN2*HH)/2.00+00
0339      AR(2,1)=Q4R/2.00+00
0340      AI(2,1)=Q4I/2.00+00
0341      AR(3,1)=Q1R+Q4R/2.00+00+Q7R/2.00+00
0342      AI(3,1)=Q1I+Q4I/2.00+00+Q7I/2.00+00
0343      AR(4,1)=Q2R
0344      AI(4,1)=Q2I
0345      AR(5,1)=Q7R/2.00+00
0346      AI(5,1)=Q7I/2.00+00
0347      AR(7,1)=Q5R
0348      AI(7,1)=Q5I

```

```

0349      AR(3,2)=Q3
0350      AR(4,2)=Q1R-Q4R/2.00+00+Q7R/2.00+00
0351      AI(4,2)=Q1I-Q4I/2.00+00+Q7I/2.00+00
0352      AR(6,2)=AR(5,1)
0353      AI(6,2)=AI(5,1)
0354      AR(8,2)=AR(7,1)
0355      AI(8,2)=AI(7,1)
0356      AR(4,3)=-AR(2,1)
0357      AI(4,3)=-AI(2,1)
0358      AR(5,3)=Q6
0359      AR(7,3)=-AR(5,1)
0360      AI(7,3)=-AI(5,1)
0361      AR(6,4)=AR(5,3)
0362      AR(8,4)=AR(7,3)
0363      AI(8,4)=AI(7,3)
0364      AR(6,5)=-AR(4,3)
0365      AI(6,5)=-AI(4,3)
0366      AR(7,5)=Q1R+Q4R/2.00+00-Q7R/2.00+00
0367      AI(7,5)=Q1I+Q4I/2.00+00-Q7I/2.00+00
0368      AR(8,5)=AR(4,1)
0369      AI(8,5)=AI(4,1)
0370      AR(7,6)=AR(3,2)
0371      AR(8,6)=Q1R-Q4R/2.00+00-Q7R/2.00+00
0372      AI(8,6)=Q1I-Q4I/2.00+00-Q7I/2.00+00
0373      AR(8,7)=-Q4R/2.00+00
0374      AI(8,7)=-Q4I/2.00+00
0375      CALL HTRIDI (NM,N,AR,AI,D,E,E2,TAU)
0376      CALL IMTQL1 (N,D,E,IERR)
0377      GO TO (170,180,190,200),I
0378      170  FREQ=O(8)-O(2)
0379      GO TO 210
0380      180  FREQ=O(7)-O(1)
0381      GO TO 210
0382      190  FREQ=O(6)-O(4)
0383      GO TO 210
0384      200  FREQ=O(5)-O(3)
0385      210  FREQ1(MM)=FREQ
0386      MM=MM+1
0387      IF(MM-28)96,96,399
0388      399  SUM=0.00+00
0389      DO 400 MM=1,28
0390      400  SUM=SUM+(FREQ1(MM)-FREQ)**2
0391      GO TO (401,407,409),K1
0392      401  SUM2=SUM
0393      IF(LL-13)402,402,403
0394      402  SUM1=SUM
0395      403  LLL=LL-12
0396      GO TO (404,404,404,405,405,405),LLL
0397      404  PP=1.00-03
0398      GO TO 406
0399      405  PP=0.50+00*(3.141590+00/180.00+00)
0400      406  P(LL)=P(LL)+PP
0401      K1=K1+1
0402      GO TO 95
0403      407  IF(SUM-SUM2)93,408,408
0404      408  P(LL)=P(LL)-2.00+00*PP
0405      K1=K1+1
0406      GO TO 95
0407      409  IF(SUM-SUM2)93,410,410
0408      410  P(LL)=P(LL)+PP
0409      93  CONTINUE
0410      IF(SUM-SUM2)411,412,412
0411      411  SUM2=SUM
0412      412  CONTINUE
0413      WRITE(6,420)SUM2
0414      420  FORMAT(' SUM2 EQUALS',F12.5)
0415      WRITE(6,430) (P(I),I=1,18)
0416      430  FORMAT('0',6F15.6)
0417      IF(SUM1-SUM2)450,450,52
0418      450  CONTINUE
0419      STOP
0420      END

```

VITA ²

Mahendrakumar G. Jani

Candidate for the Degree of

Master of Science

Thesis: ELECTRON SPIN RESONANCE STUDY OF THE E'_2 CENTER IN QUARTZ

Major Field: Physics

Biographical:

Personal Data: Born at Kanpur, Uttar Pradesh, India, August 28, 1954, the son of Gunvantrai and Manglagauri Jani.

Education: Graduated from Sainik School, Balachadi, India, in 1970; received Bachelor of Science degree in 1976 from Gujarat University; completed the requirements for the degree of Master of Science at Oklahoma State University, Stillwater, Oklahoma, in May, 1979.